
This is the **accepted version** of the article:

Matamales Andreu, Rafel; Mujal, Eudald; Galobart, Àngel; [et al.]. «Insights on the evolution of synapsid locomotion based on tetrapod tracks from the lower Permian of Mallorca (Balearic Islands, western Mediterranean)». *Palaeogeography, Palaeoclimatology, Palaeoecology*, Vol. 579 (October 2021), art. 110589. DOI 10.1016/j.palaeo.2021.110589

This version is available at <https://ddd.uab.cat/record/248974>

under the terms of the  license

1 **Insights on the evolution of synapsid locomotion based on tetrapod tracks from the lower**
2 **Permian of Mallorca (Balearic Islands, western Mediterranean)**

3 Rafel Matamales-Andreu^{1,2*}, Eudald Mujal^{1,3}, Àngel Galobart^{1,4} & Josep Fortuny¹

4
5 ¹ Institut Català de Paleontologia Miquel Crusafont, Universitat Autònoma de Barcelona, Edifici
6 ICTA-ICP, c/ Columnes s/n, Campus de la UAB, 08193 Cerdanyola del Vallès, Barcelona, Spain.

7
8 ² Museu Balear de Ciències Naturals, ctra. Palma-Port de Sóller km 30, 07100 Sóller. Mallorca,
9 Illes Balears, Spain.

10
11 ³ Staatliches Museum für Naturkunde Stuttgart, Rosenstein 1, 70191 Stuttgart, Germany.

12
13 ⁴ Museu de la Conca Dellà, c/ del Museu 4, 25650 Isona i Conca Dellà, Lleida, Spain.

14
15 *Corresponding author: rafel.matamales@icp.cat

16
17
18 **Abstract**

19 “Pelycosaur”-grade synapsids were a successful group of terrestrial tetrapods that lived
20 during the Carboniferous and Permian, utilising a wide diversity of ecological niches. They are
21 considered the trackmakers of the ichnogenera *Dimetropus* and possibly also *Dromopus* and
22 *Tambachichnium*, found in upper Palaeozoic deposits of North America, North Africa and
23 Europe. Here we describe a new morphotype from the lower Permian of Mallorca (Balearic
24 Islands, western Mediterranean), identified as cf. *Dimetropus* isp., which was purportedly
25 produced by caseid synapsids. The trackmaker identity is inferred based on the digit proportions,
26 as caseids are the only pelycosaur with species showing mesaxonic autopodia, and a relative
27 depth pattern (corresponding to the functional prevalence of the autopodia of the trackmaker)
28 showing an overall similarity to that of *Dimetropus osageorum*, which is also attributed to caseids.
29 A detailed study of the expulsion rims and drag traces makes it possible to infer the mode of
30 locomotion of the trackmaker, with a gait alternating the movement of manus and pedes of the two

31 sides of the body and lateral undulation of the spine. Our results provide new information
32 concerning the locomotion of early synapsids, which would undergo important functional
33 modifications later in their evolutionary history such as a shift from abducted to adducted posture
34 and lateral to sagittal bending of the axial skeleton.

35

36 **Key-words:** ichnology; photogrammetry; “Pelycosauria”; functional prevalence; equatorial
37 Pangaea

38

39 **1. Introduction**

40 Synapsids were a key tetrapod clade in late Palaeozoic terrestrial ecosystems, including
41 herbivores with high-fibre diet, small predators and large hypercarnivores, which occupied a
42 variety of ecological niches (Kemp, 2005; Angielczyk & Kammerer, 2018). Carboniferous and
43 Permian synapsids are nowadays included in two major clades: “pelycosaur”-grade synapsids,
44 comprising the most basal groups (Romer & Price, 1940), and non-mammalian therapsids, which
45 diversified over the middle and late Permian (Angielczyk & Kammerer, 2018). Regarding their
46 ichnological record, late Palaeozoic synapsids are represented by nine different ichnogenera, three
47 of which correspond to pelycosaurs (*Dromopus*, *Tambachichnium* and *Dimetropus*) and six to
48 therapsids (*Brontopus*, *Karooptes*, *Capitosauroides*, *Dicynodontipus*, *Dolomitipes* and
49 *Procolophonichnium*; the latter four also present in Triassic deposits) (Marchetti *et al.*, 2019a,
50 2019b, Spindler *et al.*, 2019). Some common traits of these ichnogenera (albeit not always
51 present) are the deeper impression of the median-lateral region of the tracks (median-lateral
52 functional prevalence of autopodia), tracks with paw-like shape (with faintly imprinted proximal
53 part of digits and conspicuous metatarso-/metacarpophalangeal pad and digit tip imprints) because
54 of the digital arcade of synapsid phalanges, and well-imprinted palms and soles (Marchetti *et al.*,
55 2019a; Mujal *et al.*, 2020).

56 The only ichnogenus attributed to synapsids that had been (preliminarily) reported so far
57 from the lower Permian beds of Mallorca (Balearic Islands, western Mediterranean) was
58 *Dimetropus* (Matamales-Andreu *et al.*, 2019), with forms similar to *Dimetropus leisnerianus*. The

59 present work analyses newly discovered tetrapod tracks and a trackway that correspond to a
60 second, hitherto unknown morphotype of *Dimetropus*. Those ichnites, attributable to a synapsid
61 trackmaker, possibly a caseid, enlarge the ichnofaunal diversity of the lower Permian of central
62 equatorial Pangaea, and also provide new insights on the evolution of synapsid locomotion.

63

64 **2. Geographical and geological context**

65 Mallorca is the largest of the Balearic Islands (western Mediterranean) (Figure 1A), and
66 it is broadly structured in three mountain ranges of SW–NE orientation, with rocks ranging from
67 the Carboniferous to the middle Miocene, and basins filled with sediments ranging from the upper
68 Miocene to the Holocene. The nomenclature of the Permian and Triassic lithostratigraphic units
69 of Mallorca is in need of a thorough revision, as each of the main authors who studied them
70 (Calafat, 1988; Gómez-Gras, 1993; Ramos, 1995) established different names and boundaries for
71 the units, which have never been formally described. However, such a review is beyond the scope
72 of the present work, which uses a nomenclature of correlative letters (from lowermost to
73 uppermost: A, B and C) for the three main lithostratigraphic units (Figure 1B), based on the
74 stratigraphic logs of Gómez-Gras (1993), which are herein considered to be the most exhaustive
75 of those so far published.

76 The Racó de s'Algar tracksite (Calafat *et al.*, 1986, 1986–1987; Calafat, 1988), where the
77 ichnites studied herein were discovered, corresponds to the bases of two fine-grained sandstone
78 beds located in Unit B (metre 32 of the log “E” of Calafat, 1988) (Figure 1B–C). These two beds
79 are mostly tabular, although they wedge laterally, and show climbing ripple lamination,
80 corresponding to two successive point bars of a meandering river deposit separated by a thin bed
81 of mudstones, probably representing seasonal stagnation and desiccation of the channel (Figure
82 1D–E). Their bases preserve, as natural casts, the sedimentary (large mud-cracks) and biogenic
83 (tetrapod ichnites) structures recorded on the surfaces of the underlying sandy mudstone beds,
84 which nowadays are mostly eroded. The irregularity of the ichnite-bearing surfaces, reminiscent
85 of “wrinkle structures”, points to algal mat development, which probably also contributed to the
86 mode of impression and preservation of the tracks. The succession encompassing the tetrapod

87 tracks is here interpreted as a waterhole environment, with a facies assemblage that is similar to
88 that of the seasonally-dry fluvial environments from the upper Carboniferous of Nova Scotia
89 (Falcon-Lang *et al.*, 2004, 2007). In the succession of Mallorca, such a sedimentary setting can
90 be inferred based on the presence of wave ripples developed on the channel bed, suggesting
91 stagnation of the water, and subsequent desiccation of the pool, as indicated by the large mud
92 cracks (Figure 1C, E).

93 Placed in the general framework of the Permian lithostratigraphic units of Mallorca
94 (Figure 1B), this tracksite is located in the middle–upper part of what is herein called Unit B
95 (=“Racó de s’Algar unit” of Calafat, 1988; =“Stretch a” of Gómez-Gras, 1993; =“Port des
96 Canonge unit” of Ramos, 1995), which was interpreted as a meandering river system (Calafat,
97 1988; Gómez-Gras, 1993; Ramos, 1995). This unit was dated as Permian based on the discovery
98 of moradisaurine captorhinid eureptiles, both in the form of bones (Liebrecht *et al.*, 2017) and
99 tracks (Gand *et al.*, 2010, revising the ichnites figured by Calafat *et al.*, 1986–1987). More
100 recently, Matamales-Andreu *et al.* (2019) tentatively suggested that the age could be narrowed
101 down to the lower Permian based on the presence of *Dimetropus* (possibly *D. leisnerianus*), and
102 further constrained it to the upper part of the Cisuralian (Artinskian–Kungurian) because of the
103 great abundance of tracks attributed to eureptiles (*Hyloidichnus*) and the rarity of tracks produced
104 by anamniotes (see discussion on the Artinskian–Kungurian reptile radiation by Marchetti *et al.*,
105 2015, 2019c).

106

107 **3. Material and methods**

108 Five slabs with ichnites (natural casts) from the same stratigraphic surface of the Racó de
109 s’Algar tracksite (upper ichnite-bearing bed; Figure 1C) are described in the present work. The
110 material collected *in situ* for the present study consists of a right manus imprint (DA21/15-05-
111 01), housed at the Museu de Mallorca (Palma, Mallorca, Spain, acronym DA21/15-##-##).
112 Moreover, three more slabs were found *in situ* but not collected (it was not possible, as they were
113 in the base of an unstable cliff; field acronym NA-26-##): one with a poorly preserved left manus-
114 pes set (NA-26-02), one with a poorly preserved right pes imprint (NA-26-03), and one with a

115 left manus imprint (NA-26-05). Lastly, from the Tomeu Sáez collection (private collection,
116 Binissalem, Mallorca, Spain; acronym TS-#), we have examined one slab with a trackway
117 comprising three manus-pes sets (TS-3), collected *in situ* in the early 1980s. Ichnites within a
118 same slab have been identified with correlative lowercase letters. In the preservation scale of
119 Marchetti *et al.* (2019d), most of the tracks studied herein score a 2 (good preservation), although
120 some could be attributed to 1 (intermediate preservation) or even 0 (poor preservation). Therefore,
121 and although they appear to be sensibly different from previously known ichnotaxa of this age,
122 no new ichnospecies will be defined here.

123 Digital 3D models of all the surfaces with ichnites have been produced using the
124 photogrammetry technique, mostly based on the procedure explained by Mujal *et al.* (2020).
125 Agisoft Photoscan standard version 1.1.4. (<http://www.agisoft.com>) has been used to align the
126 photographs, to create the meshes and textures, and to crop the model. MeshLab version 2016.12
127 (<http://meshlab.sourceforge.net>) has been used to clean, align, scale and measure the mesh.
128 ParaView version 4.1.0 64-bit (<http://www.paraview.org>) has been used to create the false colour-
129 coded depth maps with contours. ImageJ version 1.52d (<https://imagej.nih.gov/ij>) has been used
130 to measure the main descriptive parameters for each footprint and the trackway (see Leonardi,
131 1987; Hasiotis *et al.*, 2007), herein presented in Tables 1–2. In order to compare the tracks from
132 Mallorca to their possible trackmaker, bones of the caseid *Ennatosaurus tecton* were measured
133 on the scaled 3D model provided by Romano *et al.* (2017).

134

135 **4. Systematic palaeoichnology**

136

137 Ichnogenus *Dimetropus* Romer et Price, 1940

138

139 cf. *Dimetropus* isp.

140

141 Figures 2–3; Tables 1–2.

142

143 Studied material: DA21/15-05-01, a natural cast of a right manus imprint. NA-26-02, a
144 poorly preserved natural cast of a left manus-pes set (not collected). NA-26-03, a poorly preserved
145 natural cast of a right pes imprint (not collected). NA-26-05, a natural cast of a left manus imprint
146 (not collected). TS-3, a natural cast of a trackway with two left manus-pes sets and a right manus-
147 pes set. All from the lower Permian of the upper ichnite-bearing bed of the Racó de s'Algar
148 tracksite, Banyalbufar, Mallorca, Balearic Islands, western Mediterranean.

149 Description: Pes track semiplantigrade, pentadactyl, almost as long as wide (*ca.* 7.3–8.3
150 cm). The digit imprints are slender, strongly curved laterally (outwards) and relatively long.
151 Preservation is quite variable: in some cases, the distal parts of digits are not well imprinted
152 (especially digits II and III) (Figure 2A–B), whereas in other cases digit I seems to be imprinted
153 twice (Figures 2C, 3A). No clear claw traces have been observed on any specimen. The relative
154 length of the digit imprints is ordered as follows: V<I≈II≈IV≈III (very weakly mesaxonic) (Table
155 1). However, digit imprints are dragged, deformed and partly incomplete with mudcollapsed
156 distal ends, so it cannot be decided with certainty whether digit III is really longest, because digit
157 IV may not show its true length. The total divergence angle between digits I–V of pes tracks
158 (measured on the proximal part of the digits due to their strong distal curvature) ranges from 77°
159 to 95°. The digit imprints usually have sharp posterolateral margins, whereas their anteromedial
160 margins have gentler slopes. The sole imprint is oval, with an almost straight to weakly convex
161 posteromedial margin and a length of about 1/2 of the whole track. Metatarsophalangeal pads are
162 well impressed, especially at the bases of digits I–III. The most deeply imprinted areas of the pes
163 tracks are the metatarsophalangeal pads of digits I–III (medial functional prevalence). There is an
164 expulsion rim surrounding the pes track posterolaterally.

165 Manus track plantigrade, pentadactyl, usually slightly wider (6.9–7.1 cm) than long (6.7–
166 9.5 cm). Digit I–IV imprints are slender, relatively long and show clawed tips. The proximal parts
167 of the digit imprints are directed medially, whereas the imprints of the tips are curved laterally,
168 giving digit imprints a “hook-shaped” appearance, especially in digit III (Figures 2B–E, 3A).
169 They become thinner and gradually decrease in depth distally. Digit V imprint, which is the
170 shortest, is almost as short as digit I, slender and usually straight, although its tip is often not well

171 impressed (Figures 2B–C, 3A). Some digit imprints, especially I and II, may have drag traces in
172 front of their tips (Figure 2B–E). The relative lengths of the digit imprints are ordered as follows:
173 $V \approx I < II \approx IV < III$ (weakly mesaxonic) (Table 1). Digits radiate from the palm, usually without
174 significant overlapping, although the bases of digits I and II can be slightly superimposed. The
175 total divergence angle between the imprints of digit I–V is wide, ranging between 115° and 150°.
176 The palm imprint is posterolaterally elongated, with a concave medial margin (“lunate shape”).
177 Metacarpophalangeal pads are rounded and well-impressed, especially at the bases of digits I–IV
178 with slight overlap in I and II. The most deeply imprinted areas of the manus track are the
179 metacarpophalangeal pads of digits II–III (medial-median functional prevalence of the
180 autopodium), followed by those of digits I and IV. The imprints of the phalangeal parts of the
181 digits are shallower, with that of digit III being the deepest, followed by those of digits II and IV,
182 and then the rest of the palm. There are well-marked expulsion rims posteromedially, laterally
183 and between the imprints of digits II and III, and slightly less marked ones between the other digit
184 imprints.

185 Trackway produced by a quadrupedal animal, with pes tracks slightly larger than manus
186 tracks (weak heteropody). The manus-pes sets are alternately arranged, with the manus tracks
187 positioned at the height of the mid-proximal portion of the pes track of the next couple (Figure
188 2A). The pace angulations of the pes and the manus imprints are of about 80° and 90°,
189 respectively, and thus consistent with an abducted (sprawling) limb posture. Respect to the
190 trackway midline, pes imprints are rotated laterally (outwards) by 20–30°, whereas manus
191 imprints are rotated medially (inwards) by 9–26° and are located anteriorly from the pes imprints.
192 Manus tracks can be positioned medially or laterally from the pes tracks; this trait is variable, as
193 in other synapsid tracks (*e.g.*, Marchetti *et al.*, 2019d) The glenoacetabular distance is of about
194 32.5 cm (Table 2). No tail traces have been observed.

195

196 **5. Discussion**

197 *5.1. Comparison of cf. Dimetropus isp. from Mallorca to other Permian ichnogenera*

198 The tracks here identified as cf. *Dimetropus* isp. are pentadactyl, mesaxonic and have
199 anteroposteriorly elongated palm and sole imprints (Figure 4A), which makes it possible to rule
200 out all the Permian ichnogenera attributed to anamniotes, “reptiliomorphs”, eureptiles and
201 parareptiles (compare to Lucas, 2019), thus placing them in the synapsid group. The ichnogenera
202 currently attributed to synapsid trackmakers are: *Dromopus*, of non-varanopine varanopids and
203 some other groups of diapsids (Spindler *et al.*, 2019; Figure 4B); *Tambachichnium*, of varanopids
204 (Voigt, 2005; Marchetti *et al.*, 2019a; Figure 4C); *Dimetropus*, of edaphosaurids,
205 sphenacodontids, ophiacodontids and caseids (Voigt & Ganzelewski, 2010; Sacchi *et al.*, 2014;
206 Marchetti *et al.*, 2019a; Figure 4D–J); *Brontopus*, of dinocephalians (Marchetti *et al.*, 2019a;
207 Figure 4K–L); *Dolomitipes*, of dicynodonts (Marchetti *et al.*, 2019a; Figure 4M–N); *Karooipes*,
208 of gorgonopsians (Marchetti *et al.*, 2019a; Figure 4O); *Capitosauroides* and at least some
209 ichnospecies of *Procolophonichnium*, of therocephalians (Marchetti *et al.*, 2019a, 2019b;
210 Buchwitz *et al.*, 2020; Figure 4P–Q); and *Dicynodontipus*, of cynodonts (Marchetti *et al.*, 2019a;
211 Figure 4R).

212 Although the specimens herein identified as cf. *Dimetropus* isp. cannot readily be
213 attributed to any of these known ichnogenera (hence the open nomenclature at ichnogenus-level;
214 see Figure 4), their manus imprints are very similar to other tracks attributed to the ichnogenus
215 *Dimetropus* in the shape of the palm/sole and the digit imprints (compare to Gand, 1988: figure
216 52D; Haubold *et al.*, 1995: fig. 23A; Voigt, 2005: fig. 35D). The strong outwards rotation of the
217 pes imprint, the general proportions, the pace angulation and the stride could be also compared to
218 those of *Capitosauroides* (see Buchwitz *et al.*, 2020). The latter, however, has hitherto not been
219 found in lower Permian deposits (Buchwitz *et al.*, 2020), and thus here the assignation to
220 *Dimetropus* (in open nomenclature) is favoured.

221

222 5.2. Comparison of cf. *Dimetropus* isp. from Mallorca with other ichnospecies of *Dimetropus*

223 Sacchi *et al.* (2014) considered five valid ichnospecies within the ichnogenus
224 *Dimetropus*: *D. leisnerianus* (Geinitz, 1863), *D. osageorum* Sacchi, Cifelli, Citton, Nicosia et
225 Romano, 2014, and perhaps *D. berea* (Tilton, 1931), *D. salopensis* Haubold et Sarjeant, 1973,

226 and *D. nicolasi* Gand et Haubold, 1984. However, the last three need revision to rule out that they
227 are undertracks of *D. leisnerianus* (e.g., Voigt, 2005).

228 cf. *Dimetropus* isp. from Mallorca differs from *D. leisnerianus* (Figure 4E–F) by the
229 following features: (1) the manus imprints are weakly mesaxonic in the former, whereas in the
230 latter they are clearly ectaxonic; (2) the digit tips of the manus imprints (especially digit III) are
231 “hook-shaped” in the former, whereas they are mostly straight in the latter; (3) the digits of the
232 manus imprints of the former usually have relatively higher divergence angles than those of the
233 latter; (4) the depth of the digits of the manus imprints decreases distally in the former, whereas
234 in the latter they are deepest proximally and distally, with a shallower region in between; (5) the
235 pes imprints are rotated outwards (laterally) in the former, whereas in the latter they are
236 subparallel to the trackway midline or even slightly rotated inwards (medially); (6) the digits of
237 the pes imprint of the former are all strongly rotated outwards (laterally), whereas they are straight
238 in the former; (7) the sole imprint is anteroposteriorly short and oval in the former, whereas it is
239 usually posteriorly extended in the latter; (8) the autopodial functional prevalence inferred from
240 the relative depth pattern of the manus and pes imprints of the former is medial-median and
241 medial, respectively, whereas in the latter they are both lateral. For comparison, see tracks and
242 trackways of *D. leisnerianus* in Voigt (2005, 2012), Voigt & Ganzelewski (2010), Voigt *et al.*
243 (2011, 2012), Lucas *et al.* (2016), Mujal *et al.* (2016a, 2020), Marchetti *et al.* (2019a).

244 The material from Mallorca differs from *D. berea*, *D. salopensis* and *D. nicolasi*
245 essentially in the same characters listed above for *D. leisnerianus* (see specimens in Haubold &
246 Sarjeant, 1973; Gand & Haubold, 1984; Gand, 1988; Haubold *et al.*, 1995, Lucas *et al.*, 2016).
247 However, these three ichnospecies are of dubious validity (e.g., Voigt, 2005), with definitions
248 based on a few isolated ichnites and manus-pes sets that have slightly different digit lengths, pace
249 angulation angles and distribution of depths than those of *D. leisnerianus* (see Sacchi *et al.*, 2014).
250 Further research on the type specimens or new materials from the type localities could elucidate
251 this matter, although such a revision is beyond the scope of the present work. Moreover, cf.
252 *Dimetropus* isp. from Mallorca is also different from the Carboniferous *Dimetropus* isp. figured
253 by Voigt & Ganzelewski (2010), *Dimetropus* isp. figured by Lagnaoui *et al.* (2018) and cf.

254 *Dimetropus* isp. figured by Marchetti *et al.* (2019c), because of the reasons listed above for *D.*
255 *leisnerianus*.

256 cf. *Dimetropus* isp. from Mallorca differs from *D. osageorum* (Figure 4H) by the
257 following features: (1) the digits of the manus imprints of the former are long, slender and digit
258 III is “hook-shaped”, whereas in the latter they are straight, very short and thick; (2) the sole
259 imprints are posteriorly short in the former, whereas in the latter they are elongated, with a marked
260 medial embayment; (3) the pes imprints are strongly rotated outwards (laterally) in the former,
261 whereas in the latter they are subparallel to the trackway midline or even slightly rotated inwards
262 (medially); (4) the pes imprints are only slightly larger than the manus imprints in the former,
263 whereas the latter is notably heteropodic; (5) the functional prevalence of autopodia inferred for
264 the former is medial-median and medial, respectively for the manus and pes imprints, whereas
265 for the latter it is medial-median in both cases (see examples in Sacchi *et al.*, 2014; Romano *et*
266 *al.*, 2016, 2020).

267 It is at this point important to note that the purported *D. leisnerianus* figured by Gand
268 (1988) (Figure 4I) show a general size, proportions, heteropody and trackway parameters that are
269 comparable to those reported for *D. osageorum* by Sacchi *et al.* (2014) (Figure 4J). Their main
270 difference is that the specimens from Europe have ectaxonic tracks (although relative lengths of
271 the digit imprints appear to be very variable), whereas the North American forms have mesaxonic
272 tracks. Although this aspect is beyond the scope of the present work, future studies should
273 compare these two morphotypes to clarify whether they represent only one ichnospecies (and its
274 range of variability and extramorphological deformation) or they are distinct forms. Moreover,
275 taxonomic status of the footprints illustrated by Gand (1988) (Figure 4I) should probably be
276 reassessed, given the apparent high degree of heretopody of those tracks, atypical of *D.*
277 *leisnerianus* (Voigt, 2005; Sacchi *et al.*, 2014) (Figure 4F–H).

278

279 5.3. Trackmaker of cf. *Dimetropus* isp. from Mallorca

280 *Dimetropus* is an ichnogenus that has been attributed to various clades of “pelycosaur”-
281 grade synapsids, except for varanopids, which are considered to be the trackmakers of *Dromopus*

282 and *Tambachichnium* (see Voigt & Ganzelewski, 2010; Marchetti *et al.*, 2019a; Spindler *et al.*,
283 2019). The phylogenetic position of varanopids has recently been questioned, suggesting they are
284 actually diapsids (Ford & Benson, 2020), which would also be consistent with some of the
285 parameters of their footprints (Mujal *et al.*, 2020; Buchwitz *et al.*, 2021). However, some other
286 lines of research suggest that they are indeed more closely related to synapsids, as the morphology
287 of their maxillary canals is more similar to ophiacodonts and therapsids than to other reptiles
288 (Benoit *et al.*, 2021). Given their contentious affinities, varanopids will be not further discussed
289 here. In any case and specifically within *Dimetropus*, *D. leisnerianus* has been indistinctly
290 attributed to edaphosaurids, sphenacodontids, ophiacodontids and caseids, which have relatively
291 similar manus and pes proportions (see references in Voigt & Ganzelewski, 2010; Sacchi *et al.*,
292 2014), whereas *D. osageorum* was proposed to have been produced by large caseids or perhaps
293 edaphosaurids (Sacchi *et al.*, 2014).

294 Mujal *et al.* (2020) showed that most ichnogenera currently attributed to Carboniferous–
295 Triassic synapsid trackmakers share a median-lateral functional prevalence of the autopodia.
296 Interestingly enough, the ichnogenus *Tambachichnium*, purportedly produced by varanopids,
297 showed a different functional prevalence (median), typical of diapsids. Mujal *et al.* (2020)
298 hypothesised that the basal position of varanopids within synapsids could explain their having
299 this particular type of functional prevalence, or that it could be regarded as a trait evolved
300 convergently in a similar functionality.

301 Interestingly, the ichnospecies *D. osageorum* also appears to be at odds with the
302 hypothesis that the median-lateral functional prevalence is a trait typical of all synapsids. In the
303 touch-down phase (posterior part of the ichnite), the functional prevalence of *D. osageorum* was
304 considered to be median-lateral, but during the kick-off phase (anterior part of the ichnite) it
305 appeared to be medial-medial (Romano *et al.*, 2016, 2020). *D. osageorum* was attributed to large
306 caseid trackmakers (Sacchi *et al.*, 2014), which are also a synapsid clade that diverged before the
307 eupelycosaurs, the latter containing all ichnogenera that display a median-lateral functional
308 prevalence according to Mujal *et al.* (2020). Moreover, both manus and pes tracks of *D.*
309 *osageorum* are mesaxonic (Sacchi *et al.*, 2014), whereas the autopodia of all non-therapsid

310 eupelycosaur have a digit IV longer than III, being caseids the only pelycosaur with species
311 known to have subequal digit II–IV lengths (*e.g.*, Romer & Price, 1940; Olson, 1968).

312 In this sense, *cf. Dimetropus isp.* from Mallorca is similar to *D. osageorum* in that they
313 both share a medial-median functional prevalence (with only slight differences), especially in the
314 anterior portion of the tracks, and that they are both mesaxonic, being their digit III imprint
315 slightly longer than that of digit IV. Following the reasoning explained above, it is here tentatively
316 suggested that caseids could also be considered the trackmakers of these *cf. Dimetropus isp.*
317 tracks. Nevertheless, as noted by Sacchi *et al.* (2014), the complete structure of edaphosaurid
318 autopodia is unknown, so they cannot be fully excluded from being the trackmakers of these two
319 morphotypes of *Dimetropus*. In any case, the size of manus and pes tracks of *cf. Dimetropus isp.*
320 from Mallorca is consistent with the general proportions and dimensions of the autopodia of the
321 middle Permian genus *Ennatosaurus*, which is the only caseid of relatively small size with digits
322 III and IV being subequal in length (*e.g.*, Olson, 1968; Romano *et al.*, 2017); all other small-sized
323 genera have a digit IV that is clearly longer than III (*e.g.*, Spindler *et al.*, 2016; Berman *et al.*,
324 2020). Moreover, the manus/pes proportions (1.02 in *Ennatosaurus* and 0.83–0.95 in *cf.*
325 *Dimetropus isp.* from Mallorca) and the glenoacetabular distance in relation to the pes length
326 (4.97 in *Ennatosaurus* and 3.93–4.41 in *cf. Dimetropus isp.* from Mallorca) are also similar
327 (measurements of *Ennatosaurus* based on the complete skeleton figured by Romano *et al.*, 2017).
328 Interestingly, a partial vertebra tentatively attributed to *cf. Ennatosaurus tecton*, of notably larger
329 size than the Russian specimens, was reported from the middle Permian of the Pyrenees (Mujal
330 *et al.*, 2016b), which were palaeogeographically close to the Mallorcan basin.

331 Taking all of the above into account, a caseid identity for the trackmaker of *cf.*
332 *Dimetropus isp.* from Mallorca becomes feasible; specifically, a relatively small-sized form with
333 digits III and IV subequal in length, similar to *Ennatosaurus*. Nevertheless, further osteological
334 discoveries are needed to confirm this attribution, especially of autopodial material of more small
335 forms of caseids and also edaphosaurs.

336

337 *5.4. Locomotion of the trackmaker of cf. Dimetropus isp. from Mallorca*

338 Despite the abundant record of upper Palaeozoic ichnites (*e.g.*, Lucas, 2019), detailed
339 studies of functionality and locomotion are all relatively recent (Voigt *et al.*, 2007; Nyakatura
340 *et al.*, 2015, 2019; Romano *et al.*, 2016, 2020; Marchetti *et al.*, 2017; Buchwitz & Voigt, 2018;
341 Mujal & Marchetti, 2020; Buchwitz *et al.*, 2021; Logghe *et al.*, 2021). Therefore, although the
342 general patterns of locomotion are well understood, work remains to be done on the evolutionary
343 timing of the locomotion style of different clades. In this sense, a detailed study of the distribution
344 of trackway parameters and the depth patterns of the ichnites and associated expulsion rims makes
345 it possible to infer different phases in the step cycle and the mode of locomotion of *cf. Dimetropus*
346 *isp.* from Mallorca, thus adding new insight on the locomotion patterns of primitive “pelycosaur”-
347 grade synapsids.

348 The general functional interpretation for the manus track of *cf. Dimetropus isp.* from
349 Mallorca differs little from that offered by Romano *et al.* (2016) for *D. osageorum*. In fact,
350 expulsion rims of different height arranged around the tracks further complement this
351 interpretation. In the touch-down phase, the weight was mostly applied on the pad below the
352 ulnare, proximally to digit V (lateral functional prevalence). In the manus tracks of *cf. Dimetropus*
353 *isp.* from Mallorca, this is not only represented by a relatively deep imprint of the posterolaterally
354 part of the palm, but also by a high expulsion rim located around it (Figures 2B–E, 5A). After
355 that, the weight shifted towards the pad below the radiale and the metacarpophalangeal pads of
356 digits I, II and III (medial-median functional prevalence) during the kick-off phase, making them
357 the deepest-imprinted areas of the track (Figure 5B). Digit drag traces (Figures 2B–C, E, 5C) were
358 also formed during this phase evidencing an initial movement of the manus towards the medial-
359 anterior part.

360 The functional interpretation of the pes track of *cf. Dimetropus isp.* from Mallorca is, on
361 the other hand, quite different to that of *D. osageorum* by Romano *et al.* (2016). Possibly, the
362 most noteworthy trait of the pes tracks of *cf. Dimetropus isp.* from Mallorca is their strong lateral
363 rotation, coupled with an additional lateral curvature of the imprints of digits III–V. It is likely
364 that, during locomotion, the trackmaker used an alternate lateral bending of the trunk, as inferred
365 for other pelycosaur (Hopson, 2015). It is herein interpreted that in the touch-down phase, there

366 was an initial dragging of the tips of digits IV and V (and, to a lesser extent, III), and then the
367 weight was applied on the pad below the astragalus and the metatarsophalangeal pads of digits
368 IV and V (lateral functional prevalence), developing a moderately high expulsion rim between
369 digits IV and V, and around the posterior region of the ichnite (Figures 2A–C, 3A–B, 5D). Shortly
370 after, and as a readjustment of the body weight when the trunk was bent towards the opposite
371 side, the pes slightly rotated medially and the imprints of digits IV, V and, to a lesser extent, III,
372 became curved laterally (Figure 5G). This movement obscured the original imprints of digits III–
373 V and the posterolateral part of the sole. In the kick-off phase, the weight shifted towards the
374 anterior part of the autopodium, specifically, on the metatarsophalangeal pads of digits I and II
375 (medial functional prevalence), where the deepest impression of the track was left (Figures 2A–
376 C, 3A–B, 5E). The fact that the anteromedial margins of the pes digit imprints have a much gentler
377 slope than the posterolateral margins (Figure 2B–C) further supports that the pes was risen off the
378 ground with an anteromedial movement (Figure 5G). Drag traces of digits I (in some cases
379 imprinted twice) and II (Figures 2C, 3A, 5F) reveal an initial anterolateral movement of the pes
380 when it was taken off the ground (Figure 5H).

381 Therefore, in both the manus and the pes imprints, the functional prevalence of the
382 autopodia changed from being lateral in the touch-down phase (posterolateral region of the
383 ichnites) to being medial-median in the kick-off phase (anterior region of the ichnites, being the
384 deepest imprinted part overall), similarly to what Romano *et al.* (2016) observed in *D. osageorum*.
385 As interpreted herein, the gait would have had lateral sequence (Hildebrand, 1980), that is, the
386 sequence of movement of manus and pedes would have alternated the left and right side of the
387 body of the trackmaker (Figure 5G–I).

388

389 5.5. Notes on the evolution of synapsid locomotion

390 The particular functional prevalence inferred for these purported caseid tracks may
391 provide new insights on the evolution of the synapsid mode of locomotion. Anamniotes and basal
392 amniotes (*i.e.*, seymouriamorphs, diadectomorphs, captorhinomorphs) produced ichnites that
393 showed a medial-median functional prevalence of their autopodia (Mujal *et al.*, 2020). On the

394 other hand, eupelycosaurs, which include all the more derived synapsids, seem to homogeneously
395 feature a median-lateral functional prevalence of their autopodia (Mujal *et al.*, 2020). Therefore,
396 a transition between these two states of functional prevalence probably occurred between those
397 basal amniotes and the eupelycosaurs. Caseids, the purported trackmakers of the ichnites studied
398 here, correspond to a clade that diverged quite early in the synapsid tree (Ford & Benson, 2020).
399 Their tracks, as interpreted herein, show a mixture of lateral (posterior part) and medial-median
400 (anterior part) functional prevalence of their autopodia, which could be referred to the transitional
401 state referred above.

402 Caseids with mesaxonic autopodia, such as *Ennatosaurus* and *Cotylorhynchus*, nest
403 highly within the phylogeny of caseosaurs (Maddin *et al.*, 2008). This could appear to conflict
404 with the foregoing hypotheses, as the most derived caseids would have the “intermediate” state
405 of functional prevalence argued above, whereas small, primitive forms would not. Therefore, it
406 must be stressed that the present work does not necessarily consider mesaxony as a primitive state
407 of caseids, and the fact that two mesaxonic track morphotypes (cf. *Dimetropus* isp. from Mallorca
408 and *D. osageorum*) show a combination of posterolateral and anteromedial-median deeper areas
409 does not exclude ectaxonic tracks having a similar pattern. It must be noted, however, that the
410 relative depth patterns of small tracks attributed to *Dimetropus* have not been exhaustively
411 described in the literature so far, and in fact, they are known only from five specimens from the
412 West Midlands, the Thüringer Wald, the Massif Central and the Pyrenees (Meade *et al.*, 2016;
413 Mujal *et al.*, 2016a, 2020; Marchetti *et al.*, 2019a). Since *Dimetropus* is thought to have been
414 produced by a wide variety of “pelycosaur”-grade synapsids, it is likely that there are forms with
415 different types of relative depth patterns among the pool of specimens from different ages and
416 formations. Further research is needed to confirm this aspect, but it would be expected for a part
417 of the typical *D. leisnerianus* to show a relative depth pattern similar to that of cf. *Dimetropus*
418 isp. from Mallorca and *D. osageorum*. Especially interesting would be to assess this aspect in the
419 Carboniferous *Dimetropus* specimens (*e.g.*, Van Allen *et al.*, 2005; Voigt & Ganzelewski, 2010;
420 Meade *et al.*, 2016; Lagnaoui *et al.*, 2018; Marchetti *et al.*, 2019c), as they may show other traits

421 closer to the primitive state of synapsids, some of them already pointed out by Buchwitz *et al.*
422 (2021).

423

424 **6. Conclusions**

425 The present work describes a trackway and several isolated ichnites from the lower
426 Permian of Mallorca (Balearic Islands, western Mediterranean) identified as cf. *Dimetropus* isp.
427 This form differs from *Dimetropus leisnerianus* and allied forms because cf. *Dimetropus* isp. from
428 Mallorca has mesaxonic manus and pes imprints, the pes imprints are strongly rotated laterally
429 (outwards), and the deepest regions of both manus and pes imprints are located laterally in their
430 posterior half and medial-median in their anterior half. It differs from *Dimetropus osageorum*
431 because cf. *Dimetropus* isp. from Mallorca has long and slender manus and pes digit imprints,
432 and pes imprints that are strongly rotated laterally (outwards). It has been here suggested that the
433 trackmaker of cf. *Dimetropus* isp. from Mallorca can probably be attributed to caseid synapsids,
434 based on the proportions of the autopodia and its relative depth pattern being similar to that of *D.*
435 *osageorum*, which was also purportedly produced by caseids. The general relative depth pattern
436 (which corresponds to the functional prevalence of the autopodia of the trackmaker) of cf.
437 *Dimetropus* isp. of Mallorca, which is deeper in the lateral region of the posterior half and in the
438 medial-median region of the anterior half, appears to be transitional from the primitive state of
439 anamniotes and basal amniotes (medial-median functional prevalence), to the derived state of
440 eupelycosaur synapsids (lateral-median functional prevalence). This has important implications
441 for the evolution of the mode of locomotion throughout the synapsid line, as caseids, occupying
442 a basal position in the synapsid tree, probably produced footprints with a relative depth pattern
443 (and thus functional prevalence of the autopodia) that was intermediate between that of
444 anamniotes/basal amniotes and eupelycosaurs.

445

446 **Acknowledgements**

447 To Tomeu Sáez, who kindly let us study and make a 3D model of the trackway specimen
448 in his collection, as well as the precise indications on its discovery and exact stratigraphic position.

449 To Sebastià Matamalas for aid in fieldwork. To the reviewers, Michael Buchwitz and Hendrik
450 Klein, for their critical review of the manuscript that substantially improved it. To Prof. Howard
451 Falcon-Lang, editor, for reviewing and handling the manuscript. We acknowledge support from
452 the CERCA program (Generalitat de Catalunya, Spain). R.M.A. was supported by the predoctoral
453 grant FPU17/01922 (Ministerio de Ciencia, Innovación y Universidades, Spain). À.G. is member
454 of the consolidated research group 2017 SGR 1666 GRC (Generalitat de Catalunya, Spain). J.F.
455 is member of the consolidated research group 2017 SGR 086 GRC (Generalitat de Catalunya,
456 Spain). We acknowledge support from the project “Mallorca abans dels dinosaures: estudi dels
457 ecosistemes continentals del Permià i Triàsic amb especial èmfasi en les restes de vertebrats” (ref.
458 15 - 619/2020), based at the ICP and funded by the Departament de Cultura, Patrimoni i Política
459 Lingüística (Consell Insular de Mallorca).

460

461 **References**

- 462 Angielczyk, K.D. & Kammerer, C.F. (2018). Non-Mammalian synapsids: the deep roots of the
463 mammalian family tree. *In: Zachos, F. & Asher, R. (eds.). Mammalian Evolution,*
464 *Diversity and Systematics.* De Gruyter, 117–198.
- 465 Benoit, J.; Ford, D.P.; Miyamae, J.A. & Ruf, I. (2021). Can maxillary canal morphology inform
466 varanopid phylogenetic affinities? *Acta Palaeontologica Polonica*, 66(2): 389–393.
- 467 Berman, D.S.; Maddin, H.C.; Henrici, A.C.; Sumida, S.S.; Scott, D. & Reisz, R.R. (2020). New
468 primitive caseid (Synapsida, Caseasauria) from the early Permian of Germany. *Annals of*
469 *Carnegie Museum*, 86(1): 43–75.
- 470 Buchwitz, M. & Voigt, S. (2018). On the morphological variability of *Ichniotherium* tracks and
471 evolution of locomotion in the sistergroup of amniotes. *PeerJ*, 6:e4346.
- 472 Buchwitz, M.; Marchetti, L.; Jansen, M.; Falk, D.; Trostheide, F. & Schneider, J.W. (2020).
473 Ichnotaxonomy and trackmaker assignment of tetrapod tracks and swimming traces from
474 the middle Permian Hornburg Formation of Saxony-Anhalt (Germany). *Annales*
475 *Societatis Geologorum Poloniae*, 90: 291–320.

476 Buchwitz, M.; Jansen, M.; Renaudie, J.; Marchetti, L. & Voigt, S. (2021). Evolutionary change
477 in locomotion close to the origin of amniotes inferred from trackway data in an ancestral
478 state reconstruction approach. *Frontiers in Earth Science*, 9:674779.

479 Calafat, F. (1988). *Estratigrafía y sedimentología de la litofacies Buntsandstein de Mallorca*.
480 Bachelor's Thesis. Universitat de Barcelona. 127 pp. + 31 annexed figs.

481 Calafat, F.; Fornós, J.J.; Marzo, M.; Ramos, E. & Rodríguez-Perea, A. (1986). Icnología de
482 vertebrados de las facies Buntsandstein de Mallorca. *In: Cabrera, L. (ed.). XI Congreso*
483 *Español de Sedimentología. Libro de Resúmenes: 40.*

484 Calafat, F.; Fornós, J.J.; Marzo, M.; Ramos-Guerrero, E. & Rodríguez-Perea, A. (1986–1987).
485 Icnología de vertebrados de las facies Buntsandstein de Mallorca. *Acta Geològica*
486 *Hispanica*, 21–22: 515–520.

487 Falcon-Lang, H.J.; Rygel, M.C.; Calder, J.H. & Gibling, M.R. (2004). An early Pennsylvanian
488 waterhole deposit and its fossil biota in a dryland alluvial plain setting, Joggins, Nova
489 Scotia. *Journal of the Geological Society, London*, 161: 209–222.

490 Falcon-Lang, H.J.; Benton, M.J. & Stimson, M. (2007). Ecology of earliest reptiles inferred from
491 basal Pennsylvanian trackways. *Journal of the Geological Society, London*, 164: 1113–
492 1118.

493 Ford, D.P. & Benson, R.B.J. (2020). The phylogeny of early amniotes and the affinities of
494 Parareptilia and Varanopidae. *Nature Ecology & Evolution*, 4: 57–65.

495 Gand, G. (1988). *Les traces de vertébrés tétrapodes du Permien français: paléontologie,*
496 *stratigraphie, paléoenvironnements*. Ph.D. Thesis. Université de Bourgogne. 368 pp.

497 Gand, G. & Haubold, H. (1984). Traces de Vertèbrés tetrapodes du Permien du Bassin de Saint-
498 Afrique (Description, datation, comparaison avec celle du bassin de Lodève). *Géologie*
499 *Méditerranéenne*, 11(4): 321–348.

500 Gand, G.; De La Horra, R.; Galán-Abellán, B.; López-Gómez, J.; Barrenechea, J.F.; Arche, A. &
501 Benito, M.I. (2010). New ichnites from the Middle Triassic of the Iberian Ranges (Spain):
502 palaeoenvironmental and paleogeographical implications. *Historical Biology*, 22(1–3):
503 40–56.

- 504 Geinitz, H.B. (1863). Beiträge zur Kenntnis der organischen Überreste in der Dyas. *Neues*
505 *Jahrbuch für Mineralogie, Geologie und Paläontologie*, 1863: 385–398 + pl. III–IV.
- 506 Gómez-Gras, D. (1993). El Permotriás de las Baleares y de la vertiente mediterránea de la
507 Cordillera Ibérica y del Maestrat: Facies y Petrología Sedimentaria (Parte II). *Boletín*
508 *Geológico y Minero*, 104: 467–515.
- 509 Hasiotis, S.T.; Platt, B.F.; Hembree, D.I. & Everhart, M.J. (2007). The Trace-Fossil Record of
510 Vertebrates. In: William Miller, III (ed.). *Trace Fossils: Concepts, Problems, Prospects*.
511 Elsevier: 196–218.
- 512 Haubold, H. (1971). Ichnia Amphibiourum et Reptiliorum fossilium. In: Kuhn, O. (ed.).
513 *Handbuch der Paläoherpetologie*. Gustav Fischer Verlag, Stuttgart. 124 pp.
- 514 Haubold, H. & Sarjeant, W.A.S. (1973). Tetrapodenfährten aus den Keele und Enville Groups
515 (Permokarbon: Stefan und Autun) von Shropshire und South Staffordshire,
516 Großbritannien. *Zeitschrift für Geologische Wissenschaften*, 1: 895–933.
- 517 Haubold, H.; Hunt, A.P.; Lucas, S.G. & Lockley, M.G. (1995). Wolfcampian (Early Permian)
518 vertebrate tracks from Arizona and New Mexico. *New Mexico Museum of Natural History*
519 *and Science Bulletin*, 6: 135–165.
- 520 Hildebrand, M. (1980). The adaptive significance of tetrapod gait selection. *American Zoologist*,
521 20(1): 255–267.
- 522 Hopson, J.A. (2015). Fossils, trackways, and transitions in locomotion: a case study of
523 *Dimetrodon*. In: Dial, K.P.; Shubin, N. & Brainerd, E.L. (eds.). *Great Transformations*
524 *in Vertebrate Evolution*. University of Chicago Press, Chicago & London. 424 pp.
- 525 Kemp, T.S. (2005). *The Origin and Evolution of Mammals*. Oxford University Press, New York.
526 331 pp.
- 527 Klein, H.; Lucas, S.G. & Voigt, S. (2015). Revision of the ?Permian-Triassic tetrapod ichnogenus
528 *Procolophonichnium* Nopcsa 1923 with description of the new ichnospecies *P. lockleyi*.
529 *Ichnos*, 22: 155–176.

530 Lagnaoui, A.; Voigt, S.; Belahmira, A.; Saber, H.; Klein, H.; Hminna, A. & Schneider, J.W.
531 (2018). Late Carboniferous Tetrapod Footprints from the Souss Basin, Western High
532 Atlas Mountains, Morocco. *Ichnos*, 25(2–3), 81–93.

533 Leonardi, G. (1987). *Glossary and Manual of Tetrapod Footprint Palaeoichnology*.
534 Departamento Nacional de Produção Mineral, Brasília. 117 pp.

535 Liebrecht, T.; Fortuny, J.; Galobart, A.; Müller, J. & Sander, P.M. (2017). A large, multiple-tooth-
536 rowed captorhinid reptile (Amniota: Eureptilia) from the Upper Permian of Mallorca
537 (Balearic Islands, Western Mediterranean). *Journal of Vertebrate Paleontology*, 37(1):
538 e1251936, 1–6.

539 Logghe, A.; Mujal, E.; Marchetti, L.; Nel, A.; Pouillon, J.-M.; Giner, S.; Garrouste, R. & Steyer,
540 J.-S. (2021). *Hyloidichnus* trackways with digit and tail drag traces from the Permian of
541 Gonfaron (Var, France): New insights on the locomotion of captorhinomorph eureptiles.
542 *Palaeogeography, Palaeoclimatology, Palaeoecology*, 573: 110436.

543 Lucas, S.G. (2019). An ichnological perspective on some major events of Paleozoic tetrapod
544 evolution. *Bollettino della Società Paleontologica Italiana*, 58(3): 223–266.

545 Lucas, S.G.; Kollar, A.D.; Berman, D.S. & Henrici, A.C. (2016). Pelycosaurian-grade (Amniota:
546 Synapsida) footprints from the lower Permian Dunkard Group of Pennsylvania and West
547 Virginia. *Annals of Carnegie Museum*, 83(4): 287–294.

548 Maddin, H.C.; Sidor, C.A. & Reisz, R.R. (2008). Cranial anatomy of *Ennatosaurus tecton*
549 (Synapsida: Caseidae) from the Middle Permian of Russia and the evolutionary
550 relationships of Caseidae. *Journal of Vertebrate Paleontology*, 28: 160–180.

551 Marchetti, L.; Ronchi, A.; Santi, G.; Schirolli, P. & Conti, M.A. (2015). Revision of a classic site
552 for Permian tetrapod ichnology (Collio Formation, Trompia and Caffaro valleys, N.
553 Italy), new evidences for the radiation of captorhinomorph footprints. *Palaeogeography,*
554 *Palaeoclimatology, Palaeoecology*, 433: 140–155.

555 Marchetti, L.; Mujal, E. & Bernardi, M. (2017). An unusual *Amphisauropus* trackway and its
556 implication for understanding seymouriamorph locomotion. *Lethaia*, 50: 162–174.

557 Marchetti, L.; Belvedere, M.; Voigt, S.; Klein, H.; Castanera, D.; Díaz-Martínez, I.; Marty, D.;
558 Xing, L.; Feola, S.; Melchor, R.N. & Farlow, J.O. (2019d). Defining the morphological
559 quality of fossil footprints. Problems and principles of preservation in tetrapod ichnology
560 with examples from the Palaeozoic to the present. *Earth-Science Reviews*, 193: 109–145.

561 Marchetti, L.; Klein, H.; Buchwitz, M.; Ronchi, A.; Smith, R.M.H.; De Klerk, W.J.; Sciscio, L.
562 & Groenewald, G.H. (2019a). Permian-Triassic vertebrate footprints from South Africa:
563 Ichnotaxonomy, producers and biostratigraphy through two major faunal crises.
564 *Gondwana Research*, 72: 139–168.

565 Marchetti, L.; van der Donck, H.; van Hylckama Vlieg, M. & Doring, M.A.D. (2019b). Leaving
566 only trace fossils-the unknown visitors of Winterswijk. *Staringia*, 16: 250–257.

567 Marchetti, L.; Voigt, S.; Lucas, S.G.; Francischini, H.; Dentzien-Dias, P.; Sacchi, R.; Mangiacotti,
568 M.; Scali, S.; Gazzola, A.; Ronchi, A. & Millhouse, A. (2019c). Tetrapod ichnotaxonomy
569 in eolian paleoenvironments (Coconino and De Chelly formations, Arizona) and late
570 Cisuralian (Permian) sauropsid radiation. *Earth-Science Reviews*, 190: 148–170.

571 Marchetti, L.; Voigt, S. & Klein, H. (2019e). Revision of Late Permian tetrapod tracks from the
572 Dolomites (Trentino-Alto Adige, Italy). *Historical Biology*, 31(6): 748–783.

573 Matamales-Andreu, R.; Fortuny, J.; Mujal, E. & Galobart, À. (2019). Tetrapod tracks from the
574 Permian of Mallorca (western Mediterranean): preliminary data, biostratigraphic and
575 biogeographic inferences. *In: The Palaeontological Association, 63rd annual meeting,*
576 *15th–21st December 2019: 107.*

577 Meade, L.E.; Jones, A.S. & Butler, R.J. (2016). A revision of tetrapod footprints from the late
578 Carboniferous of the West Midlands, UK. *PeerJ*, 4: e2718.

579 Mujal, E. & Marchetti, L. (2020). *Ichniotherium* tracks from the Permian of France, and their
580 implications for understanding the locomotion and palaeobiogeography of large
581 diadectomorphs. *Palaeogeography, Palaeoclimatology, Palaeoecology*, 547:109698.

582 Mujal, E.; Fortuny, J.; Oms, O.; Bolet, A.; Galobart, À. & Anadón, P. (2016a).
583 Palaeoenvironmental reconstruction and early Permian ichnoassemblage from the NE
584 Iberian Basin (Pyrenean Basin). *Geological Magazine*, 153(4): 578–600.

585 Mujal, E.; Gretter, N.; Ronchi, A.; López-Gómez, J.; Falconnet, J.; Diez, J.B.; De la Horra, R.;
586 Bolet, A.; Oms, O.; Arche, A.; Barrenechea, J.F.; Steyer, J.-S. & Fortuny, J. (2016b).
587 Constraining the Permian/Triassic transition in continental environments: Stratigraphic
588 and palaeontological record from the Catalan Pyrenees (NE Iberian Peninsula).
589 *Palaeogeography, Palaeoclimatology, Palaeoecology*, 445: 18–37.

590 Mujal, E.; Marchetti, L.; Schoch, R.R. & Fortuny, J. (2020). Upper Paleozoic to lower Mesozoic
591 tetrapod ichnology revisited: photogrammetry and relative depth pattern inferences on
592 functional prevalence of autopodia. *Frontiers in Earth Science*, 8:248, 1–23.

593 Nyakatura, J.A.; Allen, V.R.; Lauströer, J.; Andikfar, A.; Danczak, M.; Ullrich, H.-J.; Hufenbach,
594 W.; Martens, T. & Fischer, M.S. (2015). A three-dimensional skeletal reconstruction of
595 the stem amniote *Orobates pabsti* (Diadectidae): analyses of body mass, centre of mass
596 position, and joint mobility. *PLoS ONE*, 10(9): e0137284.

597 Nyakatura, J.A.; Melo, K.; Horvat, T.; Karakasiliotis, K.; Allen, V.R.; Andikfar, A.; Andrada, E.;
598 Arnold, P.; Lauströer, J.; Hutchinson, J.R.; Fischer, M.S. & Ijspeert, A.J. (2019). Reverse-
599 engineering the locomotion of a stem amniote. *Nature*, 565: 351–355.

600 Ramos, A. (1995). Transition from alluvial to coastal deposits (Permian–Triassic) on the Island
601 of Mallorca, western Mediterranean. *Geological Magazine*, 132(4): 435–447.

602 Romano, M.; Citton, P. & Nicosia, U. (2016). Corroborating trackmaker identification through
603 footprint functional analysis: the case study of *Ichniotherium* and *Dimetropus*. *Lethaia*,
604 49: 102–116.

605 Romano, M.; Brocklehurst, N. & Fröbisch, J. (2017). The postcranial skeleton of *Ennatosaurus*
606 *tecton* (Synapsida, Caseidae). *Journal of Systematic Palaeontology*, 16(13): 1097–1122.

607 Romano, M.; Citton, P. & Nicosia, U. (2020). A review of the concepts of ‘axony’ and their
608 bearing on tetrapod ichnology. *Historical Biology*, 32(5): 611–619.

609 Romer, A.S. & Price, L.I. (1940). Review of the Pelycosauria. *Geological Society of America*
610 *Special Papers*, 28: 1–538.

- 611 Sacchi, E.; Cifelli, R.; Citton, P.; Nicosia, U. & Romano, M. (2014). *Dimetropus osageorum* n.
612 isp. from the Early Permian of Oklahoma (USA): A Trace and its Trackmaker. *Ichnos*,
613 21: 175–192.
- 614 Sevillano, A. & Barnolas, A. (2019). Mapa Geológico Digital Continuo E. 1:50.000, Zona
615 Mallorca (Zona-2210). In: GEODE. Mapa Geológico Digital continuo de España.
616 Available online at: <http://info.igme.es/visorweb/> (last accessed on 26/07/2019).
- 617 Spindler, F.; Falconnet, J. & Fröbisch, J. (2016). *Callibrachion* and *Datheosaurus*, two historical
618 and previously mis-taken basal caseosaurian synapsids from Europe. *Acta*
619 *Palaeontologica Polonica*, 61(3): 597–616.
- 620 Spindler, F.; Werneburg, R. & Schneider, J.W. (2019). A new mesenosaurine from the lower
621 Permian of Germany and the postcrania of *Mesenosaurus*: implications for early amniote
622 comparative osteology. *Paläontologische Zeitschrift*, 93: 303–344.
- 623 Tilton, J.L. (1931). Permian vertebrate tracks in West Virginia. *Bulletin of the Geological Society*
624 *of America*, 42: 547–556.
- 625 Van Allen, H.E.K.; Calder, J.H. & Hunt, A.P. (2005). The trackway record of a tetrapod
626 community in a walchian conifer forest from the Permo-Carboniferous of Nova Scotia.
627 *New Mexico Museum of Natural History and Science Bulletin*, 30: 322–332.
- 628 Voigt, S. (2005). *Die Tetrapodenichnofauna des kontinentalen Oberkarbon und Perm im*
629 *Thüringer Wald - Ichnotaxonomie, Paläoökologie und Biostratigraphie*. Cuvillier Verlag,
630 Göttingen. 308 pp.
- 631 Voigt, S. (2012). Tetrapodenfährten im Rotliegend. In: Lützner, H. & Kowalczyk, G. (eds.).
632 *Stratigraphie von Deutschland X. Rotliegend. Teil I: Innervariscische Becken*.
633 Schriftenreihe der Deutschen Gesellschaft für Geowissenschaften, 61: 161–175.
- 634 Voigt, S. & Ganzelewski, M. (2010). Toward the origin of amniotes: Diadectomorph and synapsid
635 footprints from the early Late Carboniferous of Germany. *Acta Palaeontologica*
636 *Polonica*, 55(1): 57–72.
- 637 Voigt, S.; Berman, D.S. & Henrici, A.C. (2007). First well-established track-trackmaker
638 association of paleozoic tetrapods based on *Ichniotherium* trackways and diadectid

- 639 skeletons from the Lower Permian of Germany. *Journal of Vertebrate Paleontology*,
640 27(3): 553–570.
- 641 Voigt, S.; Lagnaoui, A.; Hminna, A.; Saber, H. & Schneider, J.W. (2011). Revisional notes on
642 the Permian tetrapod ichnofauna from the Tiddas Basin, central Morocco.
643 *Palaeogeography, Palaeoclimatology, Palaeoecology*, 302: 474–483.
- 644 Voigt, S.; Niedźwiedzki, G.; Raczynski, P.; Mastalerz, K & Ptaszyński, T. (2012). Early Permian
645 tetrapod ichnofauna from the Intra-Sudetic Basin, SW Poland. *Palaeogeography*,
646 *Palaeoclimatology, Palaeoecology*, 313–314: 173–180.

647 **Figures**

648 **Figure 1.** Geographical and geological context for the Racó de s'Algar tracksite, Permian of
649 Mallorca (Balearic Islands, western Mediterranean). **A:** Simplified geological map of Mallorca
650 (based on Sevillano & Barnolas, 2019), with indication of the location of the studied site. **B:**
651 Simplified stratigraphic log of the Permian of Mallorca (thicknesses based on Gómez-Gras,
652 1993), distinguishing the three main lithostratigraphic units and indicating the location of the
653 studied site. **C:** Detailed stratigraphic log of the Racó de s'Algar tracksite, indicating the position
654 of the two track-bearing beds and the dominant sedimentary structures and fossil content. **D:** Field
655 photograph of the Racó de s'Algar tracksite with indication of the main sedimentary environments
656 and the track-bearing beds. See person for scale. **E:** Close-up photograph of the Racó de s'Algar
657 tracksite showing the two beds with ichnites. See hammer for scale (30 cm), pointed by an
658 arrowhead.

659

660 **Figure 2.** Selection of the best preserved specimens of *cf. Dimetropus* isp. studied herein, all as
661 textured 3D models, false colour-coded 3D models with contours and interpretative drawings. **A:**
662 TS-3, natural cast of a trackway with two left manus-pes sets and a right manus-pes set. **B:** Close-
663 up of the natural cast of the third manus-pes set of TS-3. **C:** Close-up of the natural cast of the
664 second manus-pes set of TS-3. **D:** NA-26-05, natural cast of a left manus imprint. **E:** DA21/15-
665 05-01, natural cast of the right manus imprint. All from the lower Permian Racó de s'Algar
666 tracksite (Mallorca, Balearic Islands, western Mediterranean), Permian.

667

668 **Figure 3.** Other specimens attributed to *cf. Dimetropus* isp., both as textured 3D models, false
669 colour-coded 3D models with contours and interpretative drawings. **A:** NA-26-02, natural cast of
670 a left manus-pes set. **B:** NA-26-03, natural cast of a right pes imprint. Both from the lower
671 Permian Racó de s'Algar tracksite (Mallorca, Balearic Islands, western Mediterranean), Permian.

672

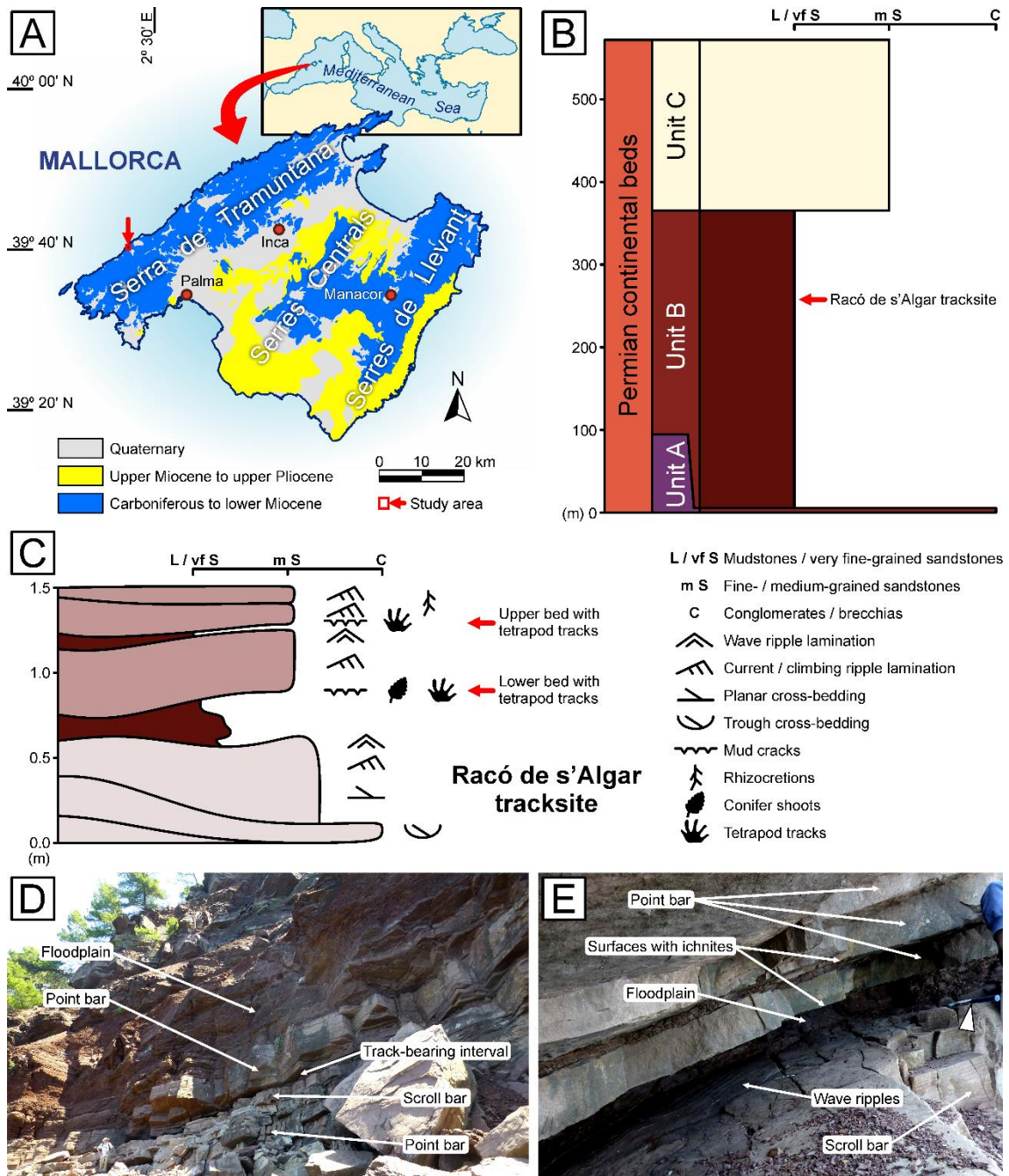
673 **Figure 4.** Schematic drawings of morphotypes of Permian and Triassic tetrapod tracks attributed
674 to non-mammalian synspsids. They are idealised and based on the best-preserved tracks, arranged

675 symmetrically in the usual trackway disposition of each form. **A:** cf. *Dimetropus* isp. from
676 Mallorca. **B:** *Dromopus lacertoides*, based on Voigt (2005) and Buchwitz *et al.* (2021). **C:**
677 *Tambachichnium schmidti*, based on Voigt (2005). **D:** *Dimetropus* isp., based on Voigt &
678 Ganzelewski (2010). **E:** cf. *Dimetropus* isp., based on Marchetti *et al.* (2019d). **F:** *Dimetropus*
679 *leisnerianus*, based on Voigt (2005). **G:** *Dimetropus leisnerianus*, based on Voigt (2005). **H:**
680 *Dimetropus leisnerianus*, based on Voigt (2005). **I:** *Dimetropus* isp., based on Gand (1988). **J:**
681 *Dimetropus osageorum*, based on Sacchi *et al.* (2014). **K:** *Brontopus antecursor*, based on Gand
682 *et al.* (2000). **L:** *Brontopus giganteus*, based on Marchetti *et al.* (2019a). **M:** *Dolomitipes accordii*,
683 based on Marchetti *et al.* (2019e). **N:** *Dolomitipes icelsi*, based on Marchetti *et al.* (2019a). **O:**
684 *Karooptes gansfonteinensis*, based on Marchetti *et al.* (2019a). **P:** *Capitosauroides bernburgensis*,
685 based on Marchetti *et al.* (2019a). **Q:** *Capitosauroides* isp., based on Buchwitz *et al.* (2020). **R:**
686 *Procolophonichnium haarmuehlensis*, based on Klein *et al.* (2015). **S:** *Dicynodontipus geinitzi*,
687 based on Marchetti *et al.* (2019a).

688

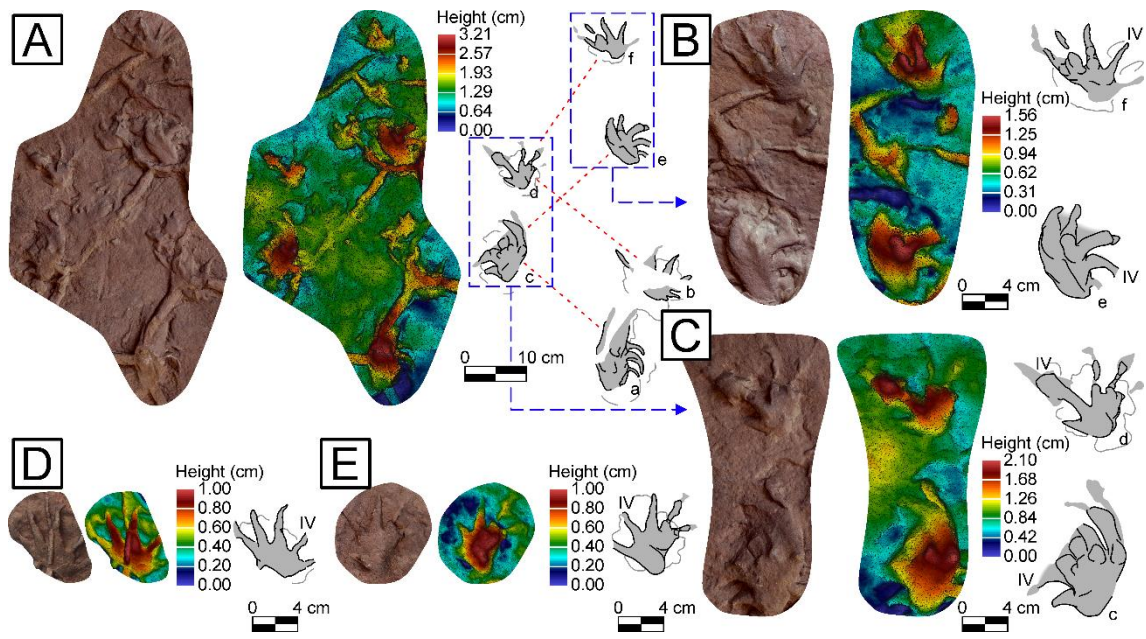
689 **Figure 5.** Functional interpretation of cf. *Dimetropus* isp. from Mallorca. **A:** Manus track in
690 touch-down phase. **B:** Manus track in kick-off phase. **C:** Manus track after the forefoot was lifted.
691 **D:** Pes track in touch-down phase. **E:** Pes track in kick-off phase. **F:** Pes track after the hindfoot
692 was lifted. **G–I:** Reconstruction of the step cycle of the trackmaker (based on *Ennatosaurus tecton*
693 illustrated by Romano *et al.*, 2017), with indication of the main movements occurring. **G:** Initial
694 phase of the step cycle, rotating the autopodia slightly medially and lining the pectoral and pelvic
695 girdles perpendicular to the body axis to gain a forward thrust. **H:** Swing phase moving the limbs
696 to the new position simultaneously to bending the trunk and finishing the movement of the girdles.
697 **I:** Final phase of the step cycle.

698 **Figure 1**



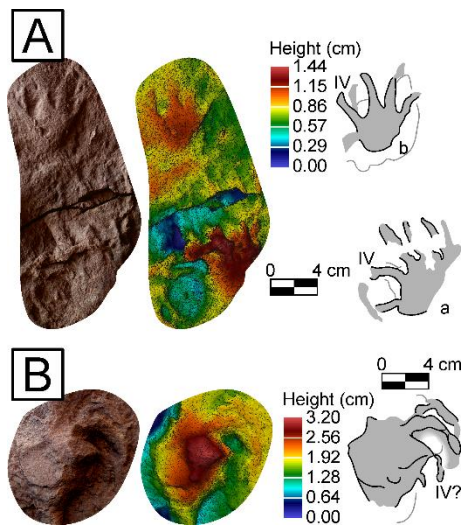
699

700 **Figure 2**

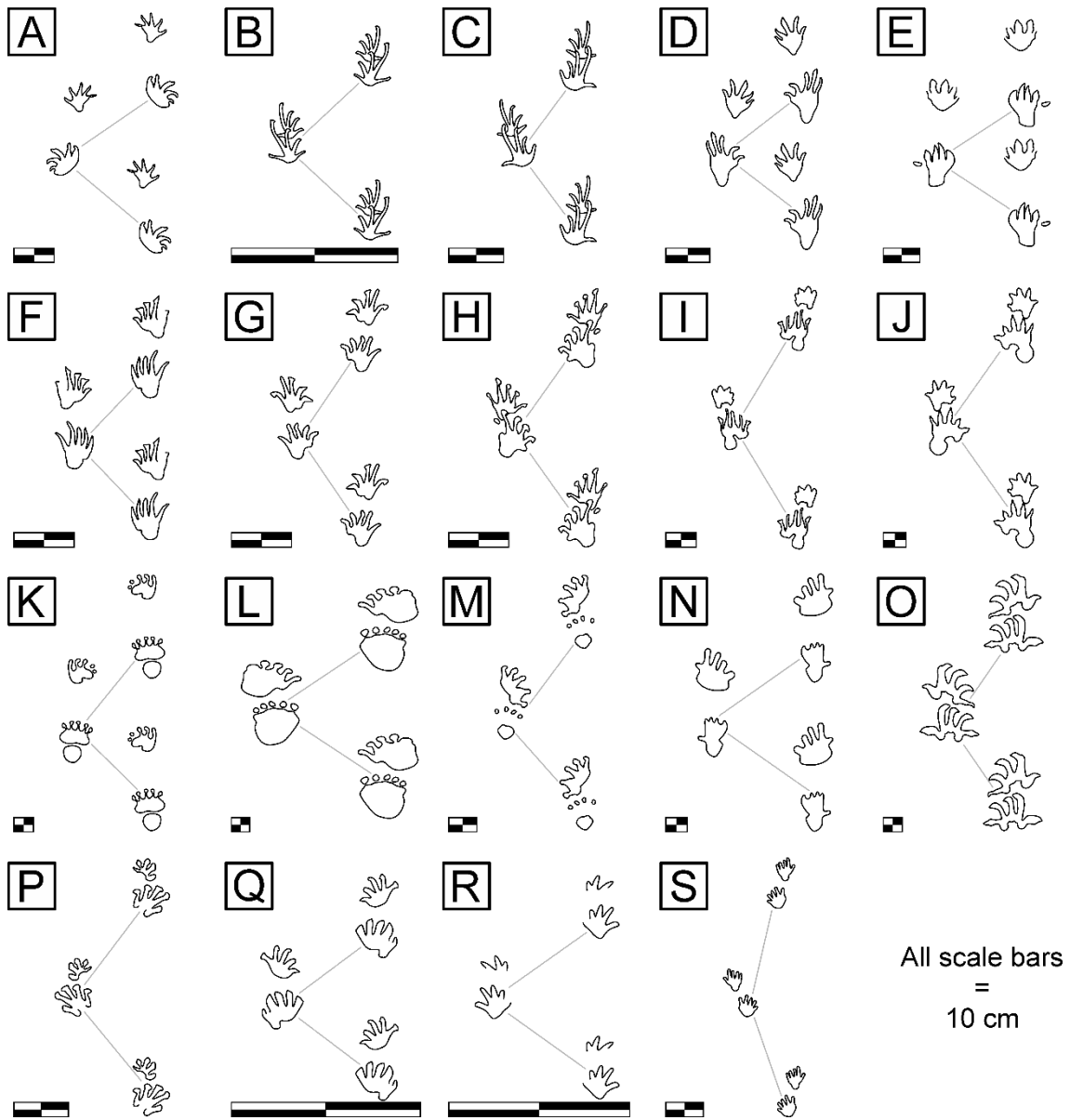


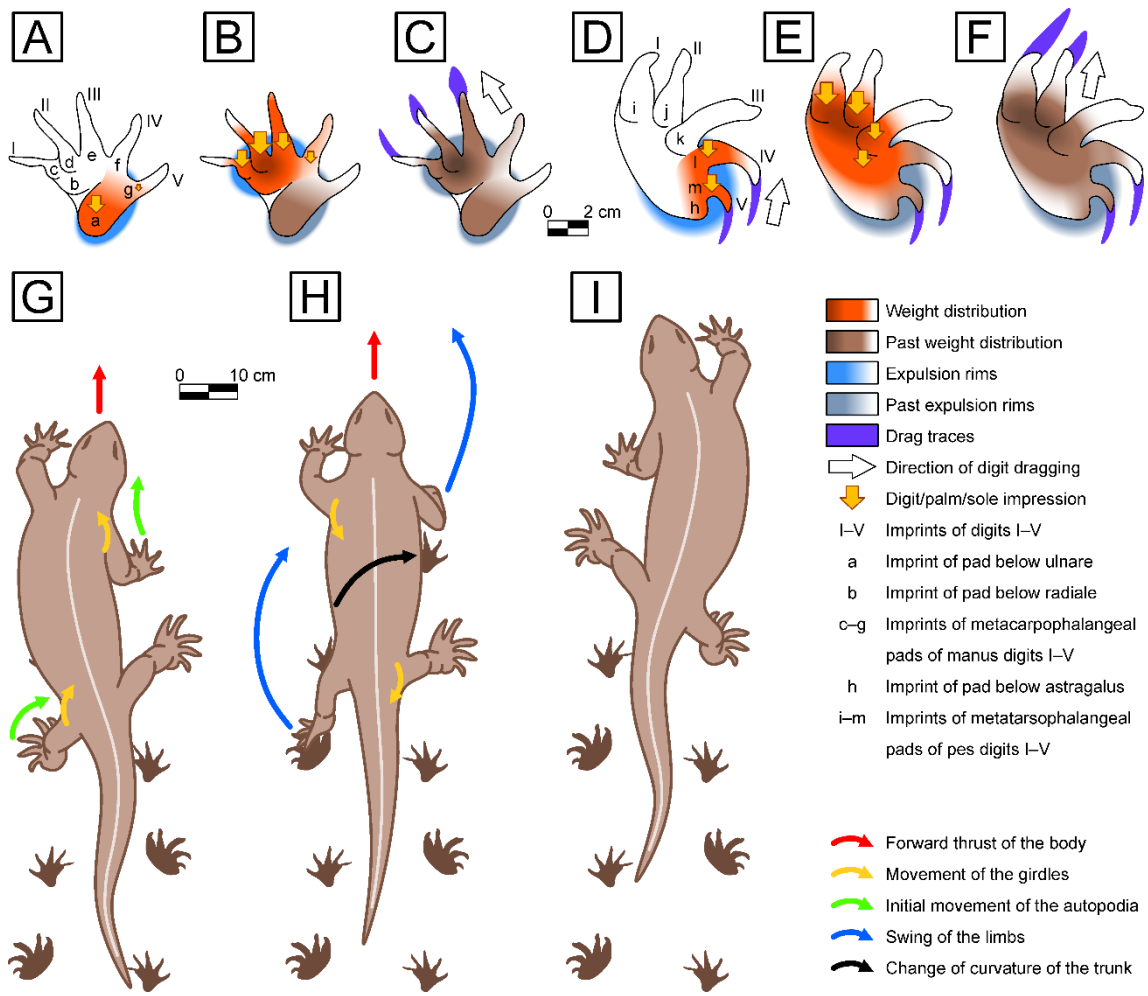
701

702 **Figure 3**



703





708 **Table 1.** Measurements taken on the studied ichnite specimens of cf. *Dimetropus* isp. from
709 Mallorca. Numbers in brackets correspond to parameters that have not been confidently measured
710 on poorly preserved ichnites. Hyphens (-) mark measurements impossible to obtain. In the
711 divarication angles, positive values correspond to ichnites rotated medially (inwards), whereas
712 negative values (-) correspond to ichnites rotated laterally (outwards).

Parameters of the TRACKS											
Slab	DA21/1 5-05-01	TS-3						NA-26-02		NA- 26- 03	NA- 26- 05
Figure	2D	2A-C						3A		3B	2E
Ichnite	-	a	b	c	d	e	f	a	b	-	-
Anatomy	Right manus	Right pes	Right manus	Left pes	Left manu s	Right pes	Right manu s	Lef t pes	Left manu s	Righ t pes	Left manu s
Length (cm)	7.14	(7.78)	(8.21)	8.27	6.86	(7.37)	7.02	-	6.66	-	6.49
Width (cm)	6.69	(13.46)	(13.15)	(8.35)	9.50	7.70	8.22	-	(7.11)	-	-
Length palm (cm)	4.03	(5.25)	-	5.57	3.83	4.17	3.77	-	3.57	-	3.93
Width palm (cm)	3.40	(8.64)	-	6.00	3.63	6.47	4.67	-	4.10	-	3.07
Length I (cm)	1.57	(5.18)	-	(4.97)	2.53	2.66	2.90	-	2.43	-	3.20
Length II (cm)	2.96	(5.68)	-	-	3.01	3.22	3.71	-	2.77	-	3.30
Length III (cm)	3.30	(2.98)	-	-	3.59	3.61	3.92	-	3.49	-	3.83
Length IV (cm)	2.57	3.79	-	4.17	(5.22)	(2.77)	3.26	-	3.00	-	-
Length V (cm)	(2.04)	2.21	2.15	2.08	(1.62)	-	2.69	-	(1.40)	-	-
Divergence angle I-II (°)	45.83	(4.18)	(63.57)	4.80	15.70	8.52	12.93	-	23.37	-	36.72
Divergence angle II-III (°)	23.42	(76.54)	-	6.32	31.38	14.60	22.58	-	14.93	-	18.68
Divergence angle III-IV (°)	40.40	(3.27)	43.91	36.01	42.44	28.24	39.31	-	35.41	-	24.26
Divergence angle IV-V (°)	37.18	(10.76)	45.08	41.51	35.98	25.86	44.45	-	68.96	-	48.03
Divergence angle I-V (°)	147.41	(95.12)	152.45	89.19	125.39	77.65	118.92	-	143.36	-	117.30
Divergence angle II-IV (°)	63.79	(80.12)	(42.06)	43.22	73.67	42.72	62.57	-	50.67	-	42.72
Divergence angle II-V (°)	101.07	(90.40)	(88.97)	84.76	110.34	68.73	106.16	-	120.00	-	91.38
Divarication from midline (°)	-	(-90.70)	(-23.03)	-31.26	9.01	-22.25	26.10	-	-	-	-

713

714

715 **Table 2.** Mean trackway measurements taken on the studied specimens of cf. *Dimetropus* isp.
 716 from Mallorca. Brackets mean that that parameter has been partially inferred. Hyphens (-) mark
 717 measurements impossible to obtain.

Parameters of the TRACKWAY					
Slab	DA21/15-05-01	TS-3	NA-26-02	NA-26-03	NA-26-05
Figure	2D	2A-C	3A	3B	2E
Pace angulation pes (°)	-	83.15	-	-	-
Pace angulation manus (°)	-	93.90	-	-	-
Stride pes (cm)	-	34.63	-	-	-
Stride manus (cm)	-	38.64	-	-	-
Pace pes (cm)	-	26.33	-	-	-
Pace manus (cm)	-	27.31	-	-	-
Length pace pes (cm)	-	17.22	-	-	-
Length pace manus (cm)	-	21.05	-	-	-
Width pace pes (cm)	-	19.57	-	-	-
Width pace manus (cm)	-	14.17	-	-	-
Interpes distance (cm)	-	12.07	-	-	-
Intermanus distance (cm)	-	6.00	-	-	-
Pes-manus distance (cm)	-	14.32	(13.12)	-	-
Width external (cm)	-	26.91	-	-	-
Width internal (cm)	-	6.00	-	-	-
Glenoacetabular distance (cm)	-	32.53	-	-	-

718